A Bidirectional Kinesin Motor in Live *Drosophila* Embryos

Catherine J. Sciambi[1], **Donald J. Komma**[1], **Helén Nilsson Sköld**[1,a], **Keiko Hirose**[2], and **Sharyn A. Endow**[1,*]

1 *Department of Cell Biology, Duke University Medical Center, Durham, NC 27710, USA*

2 *Gene Function Research Center, NIAIST, AIST Tsukuba Central 4 1-1-1 Higashi, Tsukuba, Ibaraki 305-8562, Japan*

Abstract

Spindle assembly and elongation involve poleward and away-from-the-pole forces produced by microtubule dynamics and spindle-associated motors. Here, we show that a bidirectional *Drosophila* Kinesin-14 motor that moves either to the microtubule plus or minus end *in vitro* unexpectedly causes only minor spindle defects *in vivo*. However, spindles of mutant embryos are longer than wild type, consistent with increased plus-end motor activity. Strikingly, suppressing spindle dynamics by depriving embryos of oxygen causes the bidirectional motor to show increased accumulation at distal or plus ends of astral microtubules relative to wild type, an effect not observed for a mutant motor defective in motility. Increased motor accumulation at microtubule plus ends may be due to increased slow plus-end movement of the bidirectional motor under hypoxia, caused by perturbation of microtubule dynamics or inactivation of the only other known *Drosophila* minus-end spindle motor, cytoplasmic dynein. Negative-stain electron microscopy images are consistent with highly cooperative motor binding to microtubules, and gliding assays show dependence on motor density for motility. Mutant effects of the bidirectional motor on spindle function may be suppressed under normal conditions by motor: motor interactions and minus-end movement induced by spindle dynamics. These forces may also bias wild-type motor movement toward microtubule minus ends in live cells. Our findings link motor : motor interactions to function *in vivo* by showing that motor density, together with cellular dynamics, may influence motor function in live cells.

Keywords

minus-end motor; mitosis; motor directionality; motor : motor interactions; Ncd

Spindles undergo assembly, elongation and disassembly by a dynamic interplay between poleward and away-from-the-pole forces produced by microtubule dynamics and spindle-associated microtubule motors (1,2). Poleward forces contribute to pole formation during spindle assembly (3–5), while away-from-the pole forces are needed for spindle elongation, and opposing poleward and away-from-the pole forces are required to maintain spindles and prevent their collapse (6,7).

Microtubule dynamics includes dynamic instability, the sudden rapid depolymerization or polymerization of microtubules (8), and poleward microtubule flux, slow movement of microtubules toward the poles thought to be driven by microtubule depolymerization at the poles and sliding of microtubules against one another (9–11). Microtubule depolymerization has been shown to produce sufficient force to drive poleward chromosome movement (12–14). Forces produced by microtubule polymerization, together with those produced by

microtubule depolymerization and poleward flux, may also be needed to assemble and maintain spindles.

Spindle-associated microtubule motors include cytoplasmic dynein (15,16) and motors of the kinesin family (17–19). Like other cytoskeletal motors, these motors move directionally along their filament, toward either the fast polymerizing/depolymerizing plus ends or the more stable minus ends at the nucleating center. Dynein and kinesin motors could attach spindle fibers to one another and chromosomes to spindle microtubules to assemble and maintain the meiotic or mitotic apparatus. The motors modulate microtubule dynamics and mediate spindle and chromosome dynamics (17,18,20,21). Motors could function by binding to a microtubule or kinetochore by their tail and to another microtubule by their motor domain, and move along the microtubule, sliding spindle fibers past one another or chromosomes along spindle microtubules (17,18).

Roles of specific motors in the spindle have been inferred by analysis of mutants. Early work showed that loss of function in yeast cells of two presumed plus-end Kinesin-5 (formerly BimC) (22) motors, Cin8 and Kip1, causes collapse of mitotic spindles (6) that can be suppressed by mutation of a minus-end Kinesin-14 (formerly C-terminal) motor, Kar3 (7). This has led to the idea that opposing forces are needed to maintain mitotic spindle integrity. Loss-of-function mutants have similarly been used to demonstrate that Ncd, the minus-end Kinesin-14 motor of *Drosophila*, functions in pole formation in oocyte meiotic spindles (4,5, 23,24) and attachment of centrosomes to poles in mitotic spindles (25,26). These roles are consistent with the minus-end directionality of Ncd and presence of microtubule minus ends at spindle poles, implying that directionality of movement is important to Ncd function in the spindle.

Directionality of kinesin motors is thought to be determined by the neck, immediately adjacent to the conserved motor domain (27–29). Studies of chimeric and neck-mutated motors (28, 30–34) showed that the neck plays an essential role in directionality. The neck has been proposed to function by mediating a minus-end-directed displacement of the Ncd motor along the microtubule (34,35) or by amplifying plus-end movements of the Kinesin-1 (formerly conventional kinesin) conserved motor domain (33).

Information regarding the mechanism of Ncd neck function has come from analysis of a mutant that causes the motor to move either to the microtubule plus or minus end (34). An altered neck residue in the mutant reduces interactions of the neck with the conserved motor domain. Microtubule gliding assays showed that velocity of the mutant motor was normal, but directionality was defective, resulting in gliding in either direction. Single-motor laser trap assays revealed a conformational or angle change of the motor that occurs upon motor binding to a microtubule. This movement was biased toward the minus end for wild-type Ncd but occurred in either direction for the neck mutant, indicating that the mutated neck residue is required for directional movement of Ncd to the microtubule minus end. The model that has emerged from these studies is that interactions of the neck with the conserved motor domain result in a movement, probably of the stalk/neck, that displaces the Ncd motor toward the minus end (35,36).

The importance of directionality to motor function in the spindle has been demonstrated for only a few motors that include Cin8, Kip1 and Kar3 (6,7). Because cellular dynamics could modulate motor function in ways that are presently not well understood, it is important to study motors in live cells to determine their effects *in vivo*. Here, we test the effect of altered directionality on Ncd function in the spindle by making germline transformants of the bidirectional neck mutant and analyzing live oocytes and embryos of mutant females.

Unexpectedly, our findings can be explained by effects of motor : motor interactions, together with spindle dynamics, on motor directionality and function *in vivo*.

Results

Transgenic lines expressing the bidirectional NcdNK11 motor

Ncd, the minus-end Kinesin-14 motor of *Drosophila*, functions in spindle assembly in oocytes and early embryos. To test the effects of altered directionality on motor function in the spindle, we made germline transformants expressing a mutant of Ncd, NcdNK11, a bidirectional motor that moves either toward the microtubule plus or minus end *in vitro* (34). The motor was fused to a bright variant of green fluorescent protein, S65T GFP (37), denoted GFP*, regulated by the native *ncd* promoter. Genetic tests showed that the *ncdnk11gfp** transgene rescues the frequent chromosome missegregation of *ca^{nd}*, an *ncd* null mutant deleted for the promoter and 5′ end of both *ncd* and the closely apposed *ca* gene (38). Tests of two lines, *M25M2* and *M25M3#10*, are shown in Table 1. The *M25M2* mis-segregation frequency did not differ significantly from wild type (χ^2 = 1.338, 1 df, p = 0.25). The M25M3#*10* missegregation frequency did differ significantly from wild type (χ^2 = 5.806, 1 df, p = 0.016), but the difference was small (0.87% cf 0.20%; Table 1). The *ncdnk11gfp* M25M3#10* transgene, when tested in *ncdnk11gfp* ca^{nd}*/+ females heterozygous for the transgene and *ca^{nd},* showed little or no evidence for dominant effects on meiotic and early mitotic chromosome segregation. One copy of the *ncdnk11gfp* M25M2* transgene did not fully rescue *ca^{nd}* females, but this was also observed for one copy of a wild-type *ncdgfp** transgene, *M3M1* (Table 1). Thus, the genetic tests failed to show specific loss-of-function or dominant mutant effects caused by the *ncdnk11gfp** transgene.

Live imaging of meiotic and early mitotic spindles

Ncd is a spindle motor required for spindle assembly in oocytes and centrosome attachment to poles in early embryos (4,5,23,24,26). The effects of the bidirectional motor were examined in oocytes and early embryos of *ca^{nd}* females homozygous for the *ncdnk11gfp** transgene. Analysis of meiotic spindles in live *ncdnk11gfp* M25M3#10* oocytes by laser-scanning confocal microscopy showed normal bipolar spindles (*n* = 14, total = 21) with some frayed spindles (*n* = 5) and spindles with split poles (*n* = 2) (Figure 1). Wild-type *ncdgfp* #4121* oocytes (23,26) showed normal bipolar spindles (*n* = 15, total = 17) with a few spurred or multipolar spindles (*n* = 2). The analysis indicates that meiotic spindles undergo normal assembly in *ncdnk11gfp** oocytes and do not differ significantly in overall appearance from wild-type *ncdgfp** oocytes (χ^2 = 2.358, 1 df, p = 0.125). Although defective meiotic spindles are observed in *ncdnk11gfp** oocytes, they are also observed at low frequency in wild-type *ncdgfp** oocytes. Neither *ncdnk11gfp** nor wild-type *ncdgfp** oocytes showed spindle defects as severe as those of *ca^{nd}* or other *ncd* null mutant oocytes, which frequently exhibit small, widely separated spindles associated with missegregating chromosomes (4,23,39,40).

Analysis of early cleavage spindles and division kinetics in live *ncdnk11gfp** embryos showed that both were normal. The time from microtubule nucleation in prometaphase to midbody formation in telophase of cycle 10 was not significantly different (*ncdnk11gfp* M25M2*, mean ± SEM = 263 ± 7 s, *n* = 14) or only slightly different (*ncdnk11gfp* M25M3#10*, 270 ± 8 s, *n* = 16) from wild-type *ncdgfp* #4121* embryos (253 ± 7 s, *n* = 17) (Table 2). Strikingly, the pole-to-pole length of mitotic spindles at metaphase was greater in the *ncdnk11gfp** mutant than wild type, and the difference in length increased at anaphase (Table 2). The increased spindle length is consistent with increased plus-end motor activity in the mutant that elongates the spindles by pushing the poles apart. The anaphase spindles of mutant embryos frequently appeared bent (*ncdnk11gfp* M25M2*, *n* = 43, total = 307; *ncdnk11gfp* M25M3#10*, *n* = 51, total = 276) compared with those of wild-type *ncdgfp* #4121* embryos (*n* = 25, total = 395)

($M25M2$, $\chi^2 = 11.163$, 1 df, p = 0.0008; $M25M3\#10$, $\chi^2 = 24.568$, 1 df, p < 0.0001), possibly due to unequal forces acting on the spindle fibers at anaphase. Discernible effects on mitotic spindles are thus observed in $ncdnk11gfp*$ mutant embryos, but are not as pronounced as in other ncd mutants, which show severe centrosome loss and spindle pole defects (25,26).

The genetic and cytological analyses indicate that the NcdNK11GFP* motor is expressed in $ncdnk11gfp*$ embryos and binds to spindle microtubules, but the bidirectional motor has relatively little effect on spindles in live cells compared with ca^{nd} and other loss-of-function ncd mutants. One possibility is that the plus-end motility of the bidirectional mutant is suppressed *in vivo*. To examine this possibility, we deprived embryos of oxygen to block spindle dynamics and reduce motor activity in early cleavage divisions. Under these conditions, we observed striking effects on mitotic spindles of $ncdnk11gfp*$ embryos that differed significantly from those of wild type.

Mitotic arrest in hypoxic wild-type embryos

Oxygen deprivation blocks early cleavage spindle dynamics and greatly delays or arrests cell cycle progression (41,42). Hypoxic wild-type $ncdgfp*$ #4121 embryos progressed slowly through the cell cycle or were arrested in interphase or metaphase, as reported previously. Metaphase-arrested spindles contained prominent astral microtubules with centrosomes that showed reduced NcdGFP* fluorescence (Figure 2, arrowheads). Spindles were narrow and tapered, consisting of thick bundles of brightly fluorescent fibers that terminated at the metaphase plate, differing markedly in appearance from the barrel-shaped metaphase spindles of normal embryos (Figure 2A). Antibody staining of fixed hypoxic embryos (not shown) showed the same distribution of tubulin as of the Ncd motor, although some of the motor associated with spindle microtubules is probably lost during the fixation and staining procedures. Analysis of live embryos is thus more likely to show the actual motor distribution. The tapered appearance of the metaphase-arrested spindles of oxygen-derived embryos may be caused by disassembly of the nonkinetochore spindle fibers under hypoxia, leaving the more stable kinetochore fibers and astral microtubules. The metaphase-arrested spindles showed a gap at the metaphase plate (Figure 2, arrows) corresponding to the chromosomes, which were observed in DAPI-stained fixed hypoxic embryos.

Mitotic arrest in hypoxic mutant embryos

Oxygen-deprived $ncdnk11gfp*$ mutant embryos showed delayed or arrested mitotic divisions with prominent astral microtubules and reduced centrosome fluorescence (Figure 2C,D), as observed for hypoxic wild-type embryos. The spindle fibers of hypoxic $ncdnk11gfp*$ embryos comprised thick, brightly fluorescent bundles, like the bundled spindle fibers of hypoxic wild-type $ncdgfp*$ embryos (Figure 2B). Strikingly, the astral microtubules of arrested spindles were brightly fluorescent with the NcdNK11GFP* motor and frequently appeared more brightly fluorescent at the distal or plus ends (Figures 2C,D and 3A,B,C; asterisks). Measurements showed greater motorGFP* fluorescence at the distal ends of astral microtubules of $ncdnk11gfp*$ embryos, compared with the proximal ends ($ncdnk11gfp*$ $M25M2$, $n = 314$, total = 654 microtubules from 45 spindles of eight embryos; $ncdnk11gfp*$ $M25M3\#10$, $n = 451$, total = 779 microtubules from 49 spindles of 17 embryos) (Table 3). The frequency of astral microtubules in $ncdnk11gfp*$ embryos with increased motorGFP* at the plus ends was significantly higher than in wild-type $ncdgfp*$ #4121 embryos ($n = 132$, total = 578 microtubules from 54 spindles of 11 embryos) ($M25M2$, $\chi^2 = 83.671$, 1 df, p < 0.0001; $M25M3\#10$, $\chi^2 = 165.507$, 1 df, p < 0.0001) (Table 3).

We also examined spindles of hypoxic $ncdNKgfp*$ mutant embryos that express an Ncd mutant motor that binds to microtubules but does not move on microtubules in *in vitro* gliding assays (43). The spindles of hypoxic $ncdNKgfp*$ $M5M2$ mutant embryos were delayed or arrested in

mitosis and exhibited long astral microtubules, like those of hypoxic wild-type *ncdgfp** and *ncdnk11gfp** mutant embryos. In contrast to hypoxic wild-type and *ncdnk11gfp** embryos, however, *ncdNKgfp** embryos did not show a break in fluorescence at the metaphase plate (Figure 2E), which may be due to stabilization of the spindle fibers caused by tight binding of the mutant motor to microtubules. The hypoxic *ncdNKgfp** embryos also did not show reduced centrosomal fluorescence, and the astral microtubules only infrequently showed increased motorGFP* fluorescence at the distal, compared with the proximal ends ($n = 13$, total = 214 microtubules from 23 spindles of six embryos) (Table 3). Instead, the spindle asters typically showed fluorescent centrosomes and decreasing fluorescence of astral microtubules from the proximal to the distal end (Figure 3D). These observations indicate that the diminished centrosomal fluorescence and the accumulation of motorGFP* fluorescence at the microtubule distal, or plus ends observed in hypoxic wild-type *ncdgfp** embryos, and at significantly higher frequency in hypoxic *ncdnk11gfp** embryos, is dependent on Ncd motility.

Ncd motor cooperativity

A possible explanation of the relatively minor mutant effects of the NcdNK11 bidirectional motor under normal conditions *in vivo* is that plus-end motility is suppressed by motor : motor interactions that bias directionality toward the microtubule minus end. Interactions of NcdNK11 motors with one another could cause the motors to bind cooperatively to spindle fibers and move in the same direction, influenced by spindle dynamics or the other known *Drosophila* minus-end spindle motor, cytoplasmic dynein. To test whether NcdNK11 shows cooperativity of binding to microtubules *in vitro*, motors were mixed with microtubules on a grid, negatively stained and examined using electron microscopy (EM). Grids prepared without motor showed microtubules with a pale outline of negative staining (Figure 4A). Grids of wild-type Ncd-decorated microtubules showed microtubules with a continuous dark outline (Figure 4B, top), adjacent to microtubules with a paler outline (Figure 4B, bottom). The dark outline is due to negatively stained motors bound to the surface of the microtubule and is not observed for microtubules negatively stained in the absence of motors (Figure 4A). The continuous dark outline indicates that the microtubule is fully decorated with motors along its length. These fully decorated microtubules lie adjacent to paler microtubules, which appear almost bare of motors. Grids of NcdNK11-decorated microtubules also showed fully decorated microtubules (Figure 4C, top) adjacent to microtubules that were almost bare of motors (Figure 4C, bottom). These results are consistent with cooperative binding of the Ncd and NcdNK11 motors to microtubules during grid preparation. Similar observations have been reported by others (44).

We also assayed wild-type Ncd and NcdNK11 to determine whether the motors showed density-dependent effects on motility in microtubule-gliding assays *in vitro*. The motors were fused to glutathione S-transferase (GST) to attach the motor to anti-GST antibody-coated glass surfaces. Gliding assays of motors at different densities showed slower velocity with decreasing motor density and a threshold density after which no microtubules were bound to the glass surface (Figure 5). The threshold density is a measure of the lowest motor density required to bind microtubules to the surface. The GST/NcdNK11 motor showed lower mean velocities at motor densities comparable to wild-type GST/Ncd and an approximately 2-fold higher threshold density for binding microtubules to the surface than wild-type GST/Ncd (Figure 5). These results indicate that both the NcdNK11 mutant and wild-type Ncd are dependent on interactions with other motors on the glass surface for motility in gliding assays, but the NcdNK11 motor shows a greater dependence on motor density than wild-type Ncd.

Discussion

A bidirectional spindle motor in live embryos

Directional movement of molecular motors is thought to be essential to their cellular function, permitting directed transport of cargo along actin filaments or microtubules. Here, we test the effect of altered directionality of minus-end Ncd on its function in the spindle by examining oocytes and early embryos expressing a bidirectional motor that moves either to the microtubule plus or minus end *in vitro* (34). Unexpectedly, we find that the mutant motor has little effect on meiotic or early mitotic chromosome segregation when assayed genetically, or on the cytological appearance of oocyte and early embryo spindles. The possibility that the motor is not expressed, or is unstable, is excluded by its expression as a GFP fusion protein and the observation of brightly fluorescent mitotic spindles that assemble and undergo division with kinetics similar to those of wild type. Mutant *ncdnk11gfp** oocytes showed some frayed spindles or spindles with split poles, and *ncdnk11gfp** embryos showed a higher frequency of bent anaphase spindles than wild-type *ncdgfp** embryos, and a small but significant increase in pole-to-pole length at metaphase and anaphase. These relatively minor effects indicate that the mutant motor is expressed and functional, and are consistent with abnormal, or plus-end, activity of the mutant motor. The finding that the mutant motor causes only slight effects in oocytes or embryos that otherwise lack Ncd raises the possibility that plus-end motility of the bidirectional motor is suppressed under normal conditions.

Mitotic arrest in hypoxic embryos

To test the idea that the plus-end motility of the bidirectional motor is suppressed, we blocked spindle dynamics and reduced motor activity by depriving embryos of oxygen. Hypoxic wild-type *ncdgfp** embryos were greatly delayed in cell cycle progression or arrested in interphase or metaphase, as reported previously (41,42). Arrested metaphase spindles exhibited prominent astral microtubules and thick bundles of stable microtubules that are probably kinetochore fibers. Non-kinetochore spindle fibers are less stable than kinetochore fibers (45–47) and probably disassemble under hypoxia and do not reassemble. Stabilization of kinetochore fibers could cause metaphase arrest by preventing entry into anaphase and poleward movement of chromosomes. Entry into anaphase is likely to be exquisitely sensitive to changes in microtubule dynamics. Hypoxic *ncdnk11gfp** mutant embryos showed effects similar to those of wild type with narrow, tapered metaphase-arrested spindles, thick bundles of brightly fluorescent spindle fibers, prominent astral microtubules and diminished motorGFP* fluorescence at centrosomes. The mutant motor accumulated at the distal or plus ends of astral microtubules at significantly higher frequency than in wild-type embryos, consistent with increased plus-end movement.

The effects of hypoxia on the *ncdnk11gfp** mutant embryos thus paralleled those of wild type except for the accumulation of NcdNK11GFP* at distal or plus ends of astral microtubules. Accumulation of the NcdNK11GFP* motor at astral microtubule tips can be explained by the increased ability of the NcdNK11 motor to move slowly to microtubule plus ends under hypoxic conditions *in vivo*, consistent with its movement toward plus or minus ends *in vitro* (34). This interpretation is supported by the effects observed for NcdNKGFP*, a motor that binds tightly to microtubules, but is defective in microtubule-stimulated ATPase activity and shows no microtubule motility *in vitro* (43). Spindles of hypoxic *ncdNKgfp** embryos were greatly delayed or arrested in mitosis with prominent astral microtubules, like those of wild-type *ncdgfp** and *ncdnk11gfp**. However, centrosomes were not depleted of motorGFP* fluorescence, and astral microtubules did not show frequent accumulation of fluorescence at their distal ends.

Not all of the NcdNK11GFP* accumulation observed under hypoxia was at the distal ends of microtubules – accumulation of fluorescence was also observed at astral microtubule proximal or minus ends in both wild-type *ncdgfp** and *ncdnk11gfp** spindles (Figure 3), consistent with minus-end movement of the wildtype and mutant motors. However, the motorGFP* distribution was shifted toward the microtubule plus ends in *ncdnk11gfp**, compared with *ncdgfp** spindles (Table 3). Why would hypoxia limit minus-end motor activity more dramatically than plus-end activity? This may be because there are fewer known minus-end spindle motors in *Drosophila* – only Ncd and cytoplasmic dynein – compared with the relatively large number of plus-end kinesin motors. Slow decrease of both plus- and minus-end motor activities under hypoxia might favor the perdurance of plus-end motor activity and cause NcdNK11 to switch into a plus-end mode due to motor: motor interactions (see below), revealing the plus-end activity of NcdNK11GFP*.

Another possible explanation for the increased accumulation of NcdNK11GFP* at microtubule plus ends is that the motorGFP* is transported under hypoxia to microtubule distal ends by plus-end spindle motors. We do not favor this possibility as it should result in a similar distribution of wild-type NcdGFP* and NcdNKGFP* as for NcdNK11GFP*, and this was not observed.

Our observations support the interpretation that accumulation of the wild-type NcdGFP* and NcdNK11GFP* motors at astral microtubule distal ends is due to the ability of the NcdNK11 mutant motor to move slowly toward the plus ends, as well the minus ends, under hypoxic conditions *in vivo*. This interpretation should be taken cautiously, as hypoxia can cause complex reactions in cells. Although this presumed plus-end movement was observed both for the wild-type and bidirectional NcdNK11 motors, its frequency was significantly increased for the bidirectional motor. The absence of mutant effects under normal conditions means that plus-end movement in the mitotic spindle may be suppressed under normal conditions for the NcdNK11 bidirectional motor. This is also probably true for wild-type Ncd, whose displacements are not always directed toward the minus end in laser trap assays (34).

Ncd motor : motor interactions

We asked whether the NcdNK11 motor shows a dependence on interactions with other motors for binding to microtubules and motility *in vitro*. Binding of the NcdNK11 motor to microtubules is highly cooperative, as revealed by EM of negatively stained motor-decorated microtubules showing fully decorated microtubules adjacent to nearly bare microtubules. Decoration of microtubules with motors for EM is typically done with excess motor to ensure binding by the motor to available sites on the microtubule. It is therefore unusual to observe fully decorated microtubules next to microtubules that are almost completely bare, as shown in Figure 4B,C. This indicates a high degree of cooperativity for microtubule binding by the NcdNK11 motor, which we also observed for wild-type Ncd.

Tests of Ncd and NcdNK11 dependence on density for motility by serially diluting the motor and performing gliding assays showed density dependence for maximal gliding velocity and a threshold density after which microtubules did not land and glide. These properties are characteristic of nonprocessive motors (48) and are consistent with single-motor laser trap assays demonstrating that Ncd is a nonprocessive motor (34,49). In previously reported coverslip-gliding assays, the NcdNK11 bidirectional motor showed long gliding excursions toward either the microtubule plus or minus end and occasional reversals of direction, rather than frequent switching between plus- and minus-end gliding (34), consistent with interactions between motors on the coverslip that influence directionality. This suggests that motor directionality is subject to motor : motor interactions on the coverslip and that interactions of motors arrayed along spindle fibers might suppress plus-end movement *in vivo*.

Motor cooperativity, spindle dynamics and motor directionality

The NcdNK11 motor shows evidence for cooperativity in binding to microtubules and density dependence in translocating microtubules in motility assays *in vitro*. The directional movement of NcdNK11 *in vivo* could be influenced by cooperativity of binding by the motors to spindle fibers and interactions of motors with one another after binding. Interactions of adjacent NcdNK11 motors might cause arrays of motors along spindle microtubules to move in the same direction. Spindle dynamics, including poleward flux of microtubules (9–11), and minus-end movement of cytoplasmic dynein, could bias movement of NcdNK11 toward the microtubule minus end under normal conditions, overcoming any tendency of the motor to move toward the plus end. Blocking spindle dynamics and reducing motor activity under hypoxia could cause a switch to plus-end directionality, due to a higher number of plus-end motors still active in the spindle. This would be consistent with predictions from computer modeling of increased directionality switching by lower densities of NcdNK11 motors due to cooperative effects of motors on single microtubules (50). This could explain why the plus-end directionality of NcdNK11 is suppressed under normal conditions, but revealed by hypoxia, although other effects caused by hypoxia could account for the accumulation of motorGFP* fluorescence at microtubule plus ends that we interpret as plus-end movement by the motor.

These observations suggest that spindle dynamics and other motors might also influence directionality of wild-type Ncd, whose displacements are biased toward the minus end in laser trap assays, but are not exclusively minus-end-directed (34). Our findings imply that Ncd directionality in the cell is dependent on motor density and can be influenced by interacting dynamic processes. The increased accumulation of motorGFP* at microtubule plus ends in hypoxic wild-type *ncdgfp** and *ncdnk11gfp** mutant embryos is consistent with this idea. Thus, minus-end directionality of wild-type Ncd could be rectified in live cells under normal conditions by spindle dynamics and the other known *Drosophila* minus-end spindle motor, cytoplasmic dynein, rather than being due to motor determinants alone.

Materials and Methods

Nomenclature

Kinesin proteins are referred to throughout using the new family names (22).

Transgenic lines and genetic tests

A cDNA encoding the bidirectional Ncd mutant motor, NcdNK11 N340K, fused at the C terminus to S65T GFP (37), denoted GFP*, was ligated to *pCaSpeR3* (51) and injected into *w; Δ2-3 Sb*/+ embryos. The *ncdnk11gfp** transgene is regulated by the native *ncd* promoter (38). Transformants were selected by w^+ eyecolor rescue, and lines were made homozygous for the ca^{nd} null mutant of *ncd* or heterozygous for ca^{nd} and the *TM3* balancer chromosome. Transgenic lines were analyzed by polymerase chain reaction (PCR) and DNA sequencing. Lines selected for further analysis were confirmed by molecular analysis as containing the *ncdnk11gfp** transgene with the N340K mutation and no other *ncd* gene. Homozygous *ncdnk11gfp** ca^{nd} females were tested for rescue of ca^{nd}, which causes high levels of chromosome nondisjunction and loss, as described (52). Females heterozygous for ca^{nd} and ncd^+ with one copy of the *ncdnk11gfp** transgene were tested for dominant effects, and females homozygous for ca^{nd} with one copy of the transgene were tested for haplo-insufficiency. The wild-type control for the genetic tests was Oregon R.

Transgenic lines expressing a cDNA encoding the Ncd N600K mutant, which is defective for motor movement on microtubules but not binding to microtubules or nucleotide (43), were recovered as fusions to *gfp**, as described above. The *ncdNKgfp** lines were made into stocks

with *ca^{nd}* and *TM3*, and tested by PCR and DNA sequence analysis for the presence of the mutation and absence of other *ncd* genes. Genetic tests showed failure of *ncdNKgfp** to rescue *ca^{nd}* (data not shown).

Molecular analysis of transgenic lines

DNA was prepared from one to five flies for molecular analysis of transgenic *ncdnk11gfp** and *ncdNKgfp** lines. Polymerase chain reaction was performed using primers that flank the *ncdnk11* or *ncdNK* mutations and one of the two introns present in the wild-type *ncd* gene, producing a 572-bp fragment from the cDNA transgene and a 632-bp fragment from wild-type *ncd*. The null mutant, *ca^{nd}*, contains a deletion of the promoter and 5′ end of *ncd* that includes the region corresponding to one of the primers, and thus produced no PCR fragment. Polymerase chain reaction-amplified DNA was gel purified for sequence analysis by the Duke University Comprehensive Cancer Center DNA Analysis Facility (Durham, NC, USA).

Live imaging

Spindles were examined in live oocytes and embryos produced by *ca^{nd}* females with four copies of wild-type *ncdgfp** (line *#4121: M3M1; M9F1*) (23,26), or two copies of *ncdnk11gfp** (*M25M2* or *M25M3#10*). To visualize meiotic spindles, oocytes were dissected from ovaries in Schneider's *Drosophila* medium containing 10 or 15% FCS and mounted in medium under a glass coverslip on an oxygen-permeable Teflon membrane supported by a custom metal slide (53). Meiotic spindles were imaged within 25–80 min after starting dissection to exclude changes in spindles caused by oocyte hydration. For analysis of mitosis, embryos were collected at 30-min intervals, aged on collection plates 15 min to 1 h, dechorionated, and mounted as for oocytes, but in halocarbon oil 27 (Sigma Chem. Co., St. Louis, MO, USA) instead of Schneider's medium. Live oocytes and embryos were imaged using a Bio-Rad MRC600 laser-scanning confocal microscope equipped with a 63X/1.4 NA Plan-Apochromat objective and custom GFP filter block (23,26).

Hypoxic embryos

Embryos, including those of *ncdNKgfp** (*M5M2*) *ca^{nd}* females, were collected and dechorionated as described above, then crowded closely together and mounted under a coverslip on a glass slide. Slides were aged for 1–1.5 h to allow hypoxia to develop, and embryos were imaged 1–3 h after slide preparation. In some cases the coverslip was sealed to the slide using VALAP (1:1:1 Vaseline : lanolin : paraffin, heated until clear). Fixed hypoxic embryos were stained with anti-Ncd antibodies (25,54) followed by FITC-labeled secondary antibodies and rhodamine-conjugated anti-α-tubulin antibody to label the motor and spindle microtubules, respectively, and the chromosomes were stained with DAPI. Images of the DAPI-stained chromosomes were acquired with a Princeton Instruments Penta-Max-1317-K cooled CCD camera mounted on a Leica Dialux 22 microscope using a 63X/1.4 NA Plan-Apochromat objective and overlaid on confocal images of the motor- or tubulin-labeled spindles. FITC was visualized using the Bio-Rad MRC600 confocal system and GFP filter block described above and rhodamine was visualized using a custom rhodamine filter block (568/10x excitation, Q578LP dichroic and HQ598/40 BP emission filter; Chroma Technology Corp., Rockingham, VT, USA).

Image analysis

Spindle length at metaphase and anaphase was determined by measuring from the center of one centrosome to the other using the line tool of NIH Image and time-lapse images of live, early syncytial blastoderm embryos collected under normal conditions. The distribution of motorGFP* along astral microtubules of metaphase-arrested spindles of hypoxic embryos was quantified from projections of Z-series images made using the brightest point projection

method of NIH Image. Astral microtubules were traced with the line tool to measure the pixel values along their length. Measurements were displayed as plots of greyscale value versus length and microtubules were scored as −, 0 or + for less, the same, or greater fluorescence at the distal, relative to the proximal end.

EM

Bacterially expressed, purified dimeric motor protein was mixed with microtubules on a grid in a volume of 5 μL at a concentration of 2–3 μM motor and 1–2.4 μM microtubules (tubulin dimer) in 20 mM HEPES pH 7.2, 1 mM EGTA, 5 mM MgCl$_2$, 1 mM DTT, 11–13 mM NaCl, 20 μM taxol and 1 mM AMP·PNP. Grids were negatively stained with 1% uranyl acetate and examined in a Philips Tecnai F20 electron microscope. Grids prepared with motor and microtubules but without nucleotide (with apyrase) gave similar results as with AMP·PNP, i.e. fully decorated microtubules adjacent to undecorated microtubules.

Motility assays

Microtubule-gliding assays of wild-type Ncd (MC1) (55) and NcdNK11 were performed (56) using serial dilutions of lysates prepared from cells expressing the motors as GST fusions. GST/Ncd and GST/NcdNK11 are identical except for the NK11 N340K mutation. Lysates were quantitated for GST/Ncd or GST/NcdNK11 on Western blots containing known amounts of purified GST/Ncd by cross-reaction with anti-GST antibodies. Velocities were tracked from videotapes using a custom tracking program (a gift of T Salmon and N Gliksman, University of North Carolina, Chapel Hill, NC, USA). Motor concentrations were normalized to correct for the relative amounts of wild-type Ncd and NcdNK11 in lysates used in the gliding assays.

References

1. Karsenti E, Vernos I. The mitotic spindle: a self-made machine. Science 2001;294:543–547. [PubMed: 11641489]

2. Mitchison TJ, Salmon ED. Mitosis: a history of division. Nat Cell Biol 2001;3:17–21.

3. Verde F, Berrez J-M, Antony C, Karsenti E. Taxol-induced microtubule asters in mitotic extracts of Xenopus eggs: requirement for phosphorylated factors and cytoplasmic dynein. J Cell Biol 1991;112:1177–1187. [PubMed: 1671864]

4. Hatsumi M, Endow SA. Mutants of the microtubule motor protein, nonclaret disjunctional, affect spindle structure and chromosome movement in meiosis and mitosis. J Cell Sci 1992;101:547–559. [PubMed: 1522143]

5. Matthies HJG, McDonald HB, Goldstein LSB, Theurkauf WE. Anastral meiotic spindle morphogenesis: role of the non-claret disjunctional kinesin-like protein. J Cell Biol 1996;134:455–464. [PubMed: 8707829]

6. Saunders WS, Hoyt MA. Kinesin-related proteins required for structural integrity of the mitotic spindle. Cell 1992;70:451–458. [PubMed: 1643659]

7. Hoyt MA, He L, Totis L, Saunders WS. Loss of function of Saccharomyces cerevisiae kinesin-related CIN8 and KIP1 is suppressed by KAR3 motor domain mutations. Genetics 1993;135:35–44. [PubMed: 8224825]

8. Mitchison T, Kirschner M. Dynamic instability of microtubule growth. Nature 1984;312:237–242. [PubMed: 6504138]

9. Mitchison TJ. Polewards microtubule flux in the mitotic spindle: evidence from photoactivation of fluorescence. J Cell Biol 1989;109:637–652. [PubMed: 2760109]

10. Mitchison TJ, Salmon ED. Poleward kinetochore fiber movement occurs during both metaphase and anaphase-A in newt lung cell mitosis. J Cell Biol 1992;119:569–582. [PubMed: 1400593]

11. Desai A, Maddox PS, Mitchison TJ, Salmon ED. Anaphase A chromosome movement and poleward spindle microtubule flux occur at similar rates in Xenopus extract spindles. J Cell Biol 1998;141:703–713. [PubMed: 9566970]

12. Koshland DE, Mitchison TJ, Kirschner MW. Polewards chromosome movement driven by microtubule depolymerization in vitro. Nature 1988;331:499–504. [PubMed: 3340202]

13. Lombillo VA, Nislow C, Yen TJ, Gelfand VI, McIntosh JR. Antibodies to the kinesin motor domain and CENP-E inhibit microtubule depolymerization-dependent motion of chromosomes in vitro. J Cell Biol 1995;128:107–115. [PubMed: 7822408]

14. Lombillo VA, Stewart RJ, McIntosh JR. Minus-end-directed motion of kinesin-coated microspheres driven by microtubule depolymerization. Nature 1995;373:161–164. [PubMed: 7816099]

15. Pfarr CM, Coue M, Grissom PM, Hays TS, Porter ME, McIntosh JR. Cytoplasmic dynein is localized to kinetochores during mitosis. Nature 1990;345:263–265. [PubMed: 2139717]

16. Steuer ER, Wordeman L, Schroer TA, Sheetz MP. Localization of cytoplasmic dynein to mitotic spindles and kinetochores. Nature 1990;345:266–268. [PubMed: 2139718]

17. Inoué S, Salmon ED. Force generation by microtubule assembly/disassembly in mitosis and related movements. Mol Biol Cell 1995;6:1619–1640. [PubMed: 8590794]

18. Endow SA. Microtubule motors in spindle and chromosome motility. Eur J Biochem 1999;262:12–18. [PubMed: 10231358]

19. Sharp DJ, Rogers GC, Scholey JM. Microtubule motors in mitosis. Nature 2000;407:41–47. [PubMed: 10993066]

20. Hunter AW, Wordeman L. How motor proteins influence microtubule polymerization dynamics. J Cell Sci 2000;113:4379–4389. [PubMed: 11082031]

21. Hunter AW, Caplow M, Coy DL, Hancock WO, Diez S, Wordeman L, Howard J. The kinesin-related protein MCAK is a microtubule depolymerase that forms an ATP-hydrolyzing complex at microtubule ends. Mol Cell 2003;11:445–457. [PubMed: 12620232]

22. Lawrence CJ, Dawe RK, Christie KR, Cleveland DW, Dawson SC, Endow SA, Goldstein LS, Goodson HV, Hirokawa N, Howard J, Malmberg RL, McIntosh JR, Miki H, Mitchison TJ, Okada Y, et al. A standardized kinesin nomenclature. J Cell Biol 2004;167:19–22. [PubMed: 15479732]

23. Endow SA, Komma DJ. Spindle dynamics during meiosis in Drosophila oocytes. J Cell Biol 1997;137:1321–1336. [PubMed: 9182665]

24. Endow SA, Komma DJ. Assembly and dynamics of an anastral : astral spindle: the meiosis II spindle of Drosophila oocytes. J Cell Sci 1998;111:2487–2495. [PubMed: 9701548]

25. Endow SA, Chandra R, Komma DJ, Yamamoto AH, Salmon ED. Mutants of the Drosophila ncd microtubule motor protein cause centrosomal and spindle pole defects in mitosis. J Cell Sci 1994;107:859–867. [PubMed: 8056842]

26. Endow SA, Komma DJ. Centrosome and spindle function of the Drosophila Ncd microtubule motor visualized in live embryos using Ncd-GFP fusion proteins. J Cell Sci 1996;109:2429–2442. [PubMed: 8923204]

27. Kozielski F, Sack S, Marx A, Thormählen M, Schönbrunn E, Biou V, Thompson A, Mandelkow E-M, Mandelkow E. The crystal structure of dimeric kinesin and implications for microtubule-dependent motility. Cell 1997;91:985–994. [PubMed: 9428521]

28. Sablin EP, Case RB, Dai SC, Hart CL, Ruby A, Vale RD, Fletterick RJ. Direction determination in the minus-end-directed kinesin motor ncd. Nature 1998;395:813–816. [PubMed: 9796817]

29. Endow SA. Determinants of molecular motor directionality. Nat Cell Biol 1999;1:163–167.

30. Henningsen U, Schliwa M. Reversal in the direction of movement of a molecular motor. Nature 1997;389:93–96. [PubMed: 9288974]

31. Case RB, Pierce DW, Hom-Booher N, Hart CL, Vale RD. The directional preference of kinesin motors is specified by an element outside of the motor catalytic domain. Cell 1997;90:959–966. [PubMed: 9298907]

32. Endow SA, Waligora KW. Determinants of kinesin motor polarity. Science 1998;281:1200–1202. [PubMed: 9712586]

33. Case RB, Rice S, Hart CL, Ly B, Vale RD. Role of the kinesin neck linker and catalytic core in microtubule-based motility. Curr Biol 2000;10:157–160. [PubMed: 10679326]

34. Endow SA, Higuchi H. A mutant of the motor protein kinesin that moves in both directions on microtubules. Nature 2000;406:913–916. [PubMed: 10972296]

35. Yun M, Bronner CE, Park C-G, Cha S-S, Park H-W, Endow SA. Rotation of the stalk/neck and one head in a new crystal structure of the kinesin motor protein, Ncd. EMBO J 2003;22:5382–5389. [PubMed: 14532111]

36. Higuchi H, Endow SA. Directionality and processivity of molecular motors. Curr Opin Cell Biol 2002;14:50–57. [PubMed: 11792544]

37. Heim R, Cubitt AB, Tsien RY. Improved green fluorescence. Nature 1995;373:663–664. [PubMed: 7854443]

38. Yamamoto AH, Komma DJ, Shaffer CD, Pirrotta V, Endow SA. The claret locus in Drosophila encodes products required for eye-color and for meiotic chromosome segregation. EMBO J 1989;8:3543–3552. [PubMed: 2479546]

39. Wald H. Cytologic studies on the abnormal development of the eggs of the claret mutant type of Drosophila simulans. Genetics 1936;21:264–281. [PubMed: 17246793]

40. Kimble M, Church K. Meiosis and early cleavage in Drosophila melanogaster eggs: effects of the claret-non-disjunctional mutation. J Cell Sci 1983;62:301–318. [PubMed: 6413518]

41. Foe VE, Alberts BM. Reversible chromosome condensation induced in Drosophila embryos by anoxia: visualization of interphase nuclear organization. J Cell Biol 1985;100:1623–1636. [PubMed: 3921555]

42. DiGregorio PJ, Ubersax JA, O'Farrell PH. Hypoxia and nitric oxide induce a rapid, reversible cell cycle arrest of the Drosophila syncytial divisions. J Biol Chem 2001;276:1930–1937. [PubMed: 11054409]

43. Song H, Endow SA. Decoupling of nucleotide- and microtubule-binding in a kinesin mutant. Nature 1998;396:587–590. [PubMed: 9859995]

44. Wendt TG, Volkmann N, Skiniotis G, Goldie KN, Müller J, Mandelkow E, Hoenger A. Microscopic evidence for a minus-end-directed power stroke in the kinesin motor ncd. EMBO J 2002;21:5969–5978. [PubMed: 12426369]

45. Cassimeris L, Rieder CL, Rupp G, Salmon ED. Stability of microtubule attachment to metaphase kinetochores in PtK1 cells. J Cell Sci 1990;96:9–15. [PubMed: 2197288]

46. Hyman AA, Mitchison TJ. Modulation of microtubule stability by kinetochores in vitro. J Cell Biol 1990;110:1607–1616. [PubMed: 2186046]

47. Zhai Y, Kronebusch PJ, Borisy GG. Kinetochore microtubule dynamics and the metaphase-anaphase transition. J Cell Biol 1995;131:721–734. [PubMed: 7593192]

48. Howard J. Mechanics of Motor Proteins and the Cytoskeleton. Sinauer Associates, Inc. Sunderland, MA; 2001.

49. deCastro MJ, Fondecave RM, Clarke LA, Schmidt CF, Stewart RJ. Working strokes by single molecules of the kinesin-related microtubule motor ncd. Nat Cell Biol 2000;2:724–729. [PubMed: 11025663]

50. Badoual M, Jülicher F, Prost J. Bidirectional cooperative motion of molecular motors. Proc Natl Acad Sci USA 2002;99:6696–6701. [PubMed: 12011432]

51. Thummel CS, Boulet AM, Lipshitz HD. Vectors for Drosophila P-element-mediated transformation and tissue culture transfection. Gene 1988;74:445–456. [PubMed: 3246353]

52. Komma DJ, Horne AS, Endow SA. Separation of meiotic and mitotic effects of claret nondisjunctional on chromosome segregation in Drosophila. EMBO J 1991;10:419–424. [PubMed: 1825056]

53. Davis I, Girdham CH, O'Farrell PH. A nuclear GFP that marks nuclei in living Drosophila embryos; maternal supply overcomes a delay in the appearance of zygotic fluorescence. Dev Biol 1995;170:726–729. [PubMed: 7649398]

54. Hatsumi M, Endow SA. The Drosophila ncd microtubule motor protein is spindle-associated in meiotic and mitotic cells. J Cell Sci 1992;103:1013–1020. [PubMed: 1487485]

55. Chandra R, Salmon ED, Erickson HP, Lockhart A, Endow SA. Structural and functional domains of the Drosophila ncd microtubule motor protein. J Biol Chem 1993;268:9005–9013. [PubMed: 8473343]

56. Song H, Golovkin M, Reddy ASN, Endow SA. In vitro motility of AtKCBP, a calmodulin-binding kinesin protein of Arabidopsis. Proc Natl Acad Sci USA 1997;94:322–327. [PubMed: 8990207]
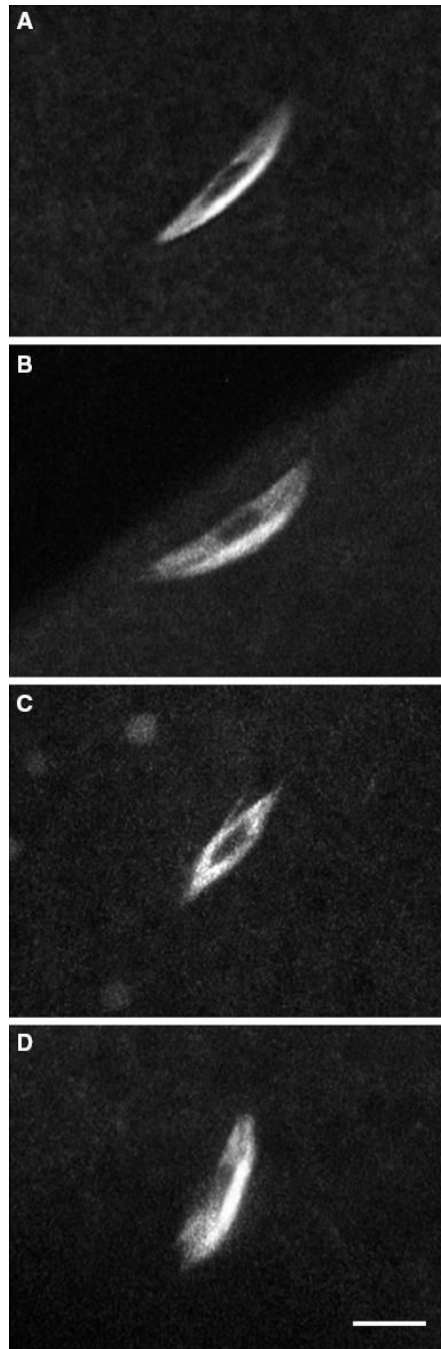
Figure 1. Meiosis I spindles in live wild-type and mutant oocytes
A) Metaphase-arrested meiosis I spindle from a wild-type *ncdgfp* #4121* oocyte. The dark
region in the middle of the spindle corresponds to the condensed meiotic chromosomes. B–D)
Meiosis I spindles from *ncdnk11gfp* M25M3#10* mutant oocytes showing (B) normal and (C)
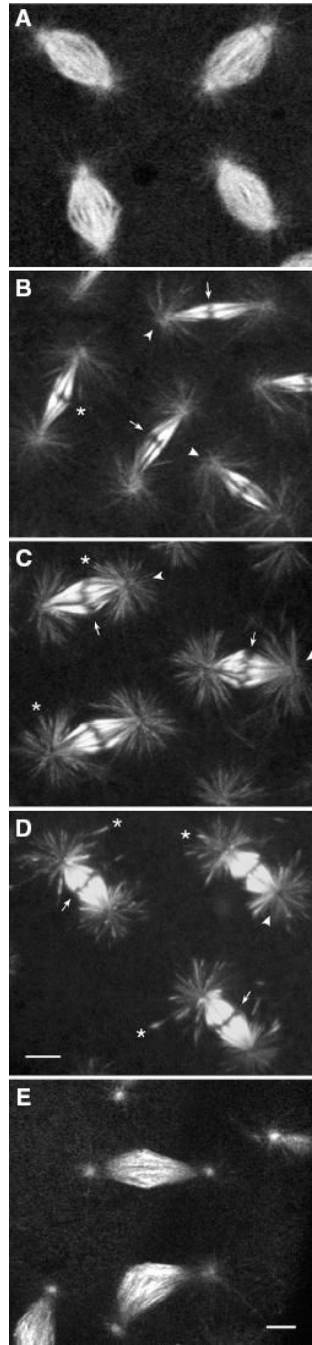frayed spindles and (D) a spindle with a split pole. Bar, 5 μm.

Figure 2. Mitotic spindles of hypoxic embryos
A) Metaphase spindles in a normal cycle 10 wild-type *ncdgfp* #4121* embryo. B–E) Metaphase-arrested spindles from hypoxic (B) wild-type *ncdgfp* #4121*, (C) *ncdnk11gfp* M25M2*, (D) *ncdnk11gfp* M25M3#10* and (E) *ncdNKgfp* M5M2* embryos. The arrested spindles of hypoxic wild-type *ncdgfp** and *ncdnk11gfp** embryos show reduced centrosomal fluorescence (arrowheads), a gap at the metaphase plate (arrows) corresponding to the chromosomes, and accumulation of motorGFP* at distal ends of astral microtubules (asterisks). These features are not observed in arrested spindles of hypoxic *ncdNKgfp** embryos. Bars, 5 μm.
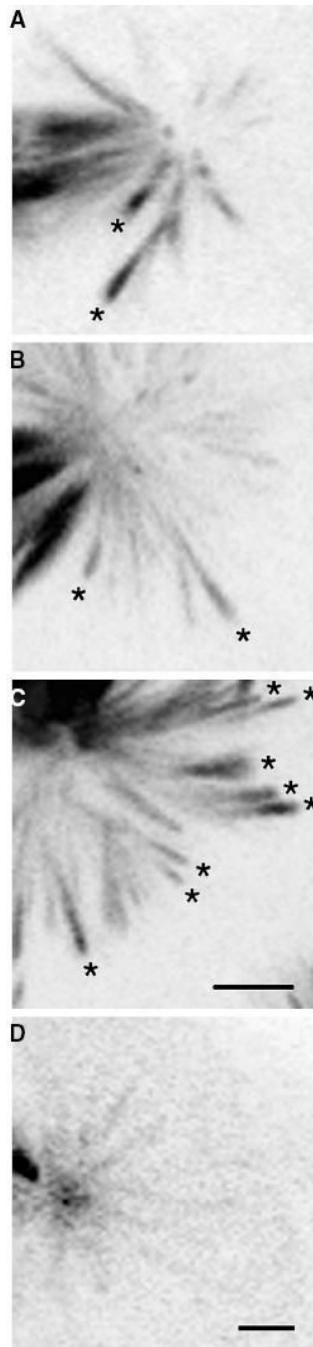
Figure 3. Accumulation of motorGFP* at distal ends of astral microtubules in spindles of hypoxic embryos
Spindles of A) wild-type *ncdgfp* #4121*, B) *ncdnk11gfp* M25M2*, C) *ncdnk11gfp* M25M3#10* and D) *ncdNKgfp* M5M2* embryos. Fluorescence along the astral microtubules was measured using NIH Image from projections of Z-series stacks. Images are shown with pixel values inverted. Microtubules with brighter fluorescence at the distal, relative to the proximal end (asterisks), were observed in both wild-type and mutant hypoxic embryos but occurred at significantly higher frequency in *ncdnk11gfp** mutant embryos. These microtubules were observed at much lower frequency in *ncdNKgfp* M5M2* spindles, which also did not show depletion of motorGFP* fluorescence from centrosomes. Bars, 2.5 μm.
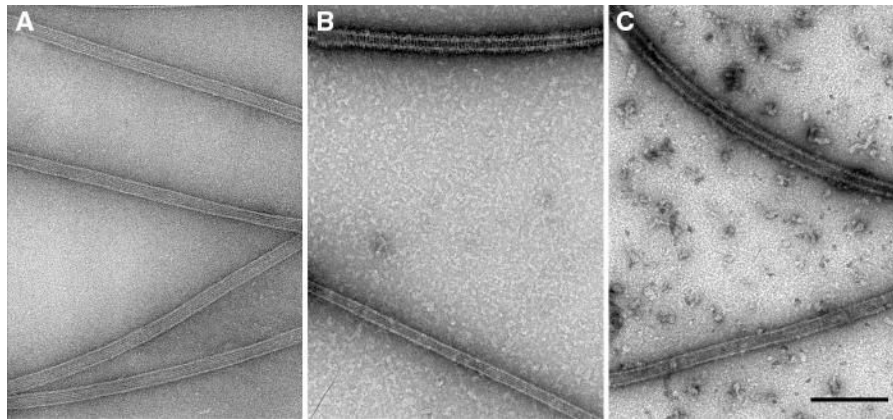
Figure 4. Motor binding to microtubules
A) Microtubules alone. Microtubules negatively stained without motors have a pale outline of negative stain. B) Wild-type Ncd bound to microtubules. Two microtubules are shown after incubation with excess wild-type Ncd motor protein, negative staining and visualization by electron microscopy (EM). One microtubule (top) appears fully decorated with motors, as indicated by the continuous dark outline; the other (bottom) with a paler outline appears almost bare of motors. C) NcdNK11 bound to microtubules. Microtubules incubated with the NcdNK11 mutant motor are fully decorated (top) or almost bare (bottom), as observed for wild-type Ncd. Bar, 0.2 μm.
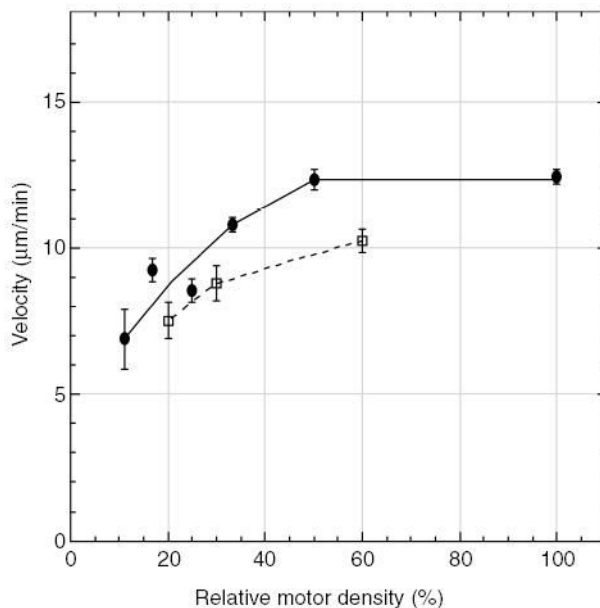
Figure 5. Dependence of gliding velocity on motor density
Velocity of microtubule gliding in assays of serially diluted GST/Ncd (•) or GST/NcdNK11
(□). Each point represents the mean microtubule gliding velocity at the indicated dilution
(average number of microtubules tracked = 22 at each dilution; error bars, ±SEM). The first
point to the left for each motor indicates the threshold density, the lowest density at which
microtubules still bound to the surface and moved. Motor concentrations were normalized to
correct for the relative amount of GST/Ncd or GST/NcdNK11 in the lysates, as determined
using Western blot analysis. The motor density at 100% is approximately 49 280 molecules/
μm^2.

Table 1

Genetic effects of *ncdnk11* on chromosome distribution. Females of the indicated genotypes were mated to tester males to determine whether *ncdnk11gfp** rescues *ca^{nd}*, an *ncd* deletion null mutant, for chromosome missegregation and embryo inviability. Chromosome mis-segregation is X chromosome meiotic nondisjunction and loss, and mitotic loss. Data for *ca^{nd}/ca^{nd}* females are from (25)

Female parent	Normal gametes	Abnormal gametes	Chromosome missegregation (%)
+/+	2018	4	0.20
ncdnk11gfp* M25M2 ca^{nd}/ncdnk11gfp* M25M2 ca^{nd}	1910	8	0.42
ncdnk11gfp* M25M3#10 ca^{nd}/ncdnk11gfp* M25M3#10 ca^{nd}	573	5	0.87
ncdnk11gfp* M25M3#10 ca^{nd}/+	2076	2	0.10
+/ca^{nd}	1190	0	0
Wild-type *ncdgfp* M3M1; ca^{nd}/ca^{nd}*	1298	163	11.2
ncdnk11gfp* M25M2; ca^{nd}/ca^{nd}	1714	60	3.38
ca^{nd}/ca^{nd}	112	69	38.1

Table 2

Effects of NcdNK11 on mitotic spindles. Females were homozygous for ca^{nd} and the wild-type *ncdgfp** and the *ncdgfp** or *ncdnk11gfp** transgene. Time is microtubule nucleation in prometaphase to midbody formation in telophase; s, seconds. M to A, spindle length increase from metaphase to late anaphase, just prior to midbody formation. Values = mean ± SEM

| | Time (s) | Pole-to-pole spindle length (µm, $n = 47$) | | | |
		Interphase	Metaphase	Anaphase	M to A
Wild-type *ncdgfp** #4121	253 ± 7 ($n = 17$)	9.5 ± 0.2	12.3 ± 0.1	15.7 ± 0.1	3.4 ± 0.1
ncdnk11gfp* M25M2	263 ± 7 ($n = 14$)	10.1 ± 0.2	12.6 ± 0.2	16.7 ± 0.2	4.1 ± 0.1
ncdnk11gfp* M25M3#10	270 ± 8 ($n = 16$)	10.3 ± 0.1	13.1 ± 0.1	17.9 ± 0.2	4.8 ± 0.1

Table 3

Distribution of fluorescence on astral microtubules of hypoxic embryos. Fluorescence of motorGFP* was measured along the length of astral microtubules of mitotic spindles. Microtubules were scored as −, 0 or + for less, the same, or greater fluorescence at the distal, compared with the proximal end. The percentage of each class is shown in parentheses

	Embryos	Spindles	Microtubules			
			−	0	+	Total
Wild-type *ncdgfp* #4121	11	54	400 (69)	46 (8)	132 (23)	578
ncdnk11gfp M25M2	8	45	262 (40)	78 (12)	314 (48)	654
ncdnk11gfp M25M3#10	17	49	292 (37)	36 (5)	451 (58)	779
ncdNKgfp M5M2	6	23	183 (86)	18 (8)	13 (6)	214